

## Stability analysis of a roadside slope in Xinjiang under the influence of construction disturbance

Bo Sha <sup>1</sup>, Bangxin Zhang <sup>2</sup>, Fan Yang <sup>1</sup>, Ningyang Feng <sup>1</sup>, Xiaogang Liu <sup>1</sup>,  
Hui Wu <sup>1</sup>, Lei Qi <sup>1</sup>, Dongming Peng <sup>2</sup>, Ziyang Huang <sup>2</sup>, Hongwei Li <sup>2</sup>  
and Chunyu Long <sup>2</sup>

<sup>1</sup> Xin Jiang Road & Bridge Construction Group Co., Ltd. Wulumuqi 830000, China;

<sup>2</sup> China Merchants Chongqing Communications Technology Research & Design Institute Co., Ltd.  
Chongqing 400067, China.

**Abstract.** Affected by continuous construction disturbance, the stability coefficient of a slope is calculated to be 0.95, which does not meet the requirements of slope stability; in order to prevent slope destabilization and damage, two kinds of reinforcement schemes are formulated, scheme 1 is “circular anti-slip pile + anchor + cut-off drainage”, scheme 2 is “square anti-slip pile + cut-off drainage”. Numerical analysis of the stress field, displacement field and stability coefficient changes of the two reinforcement schemes; the study shows that: 1) Scheme 1 and 2 both meet the requirements for slope stabilization, improving the slope stability coefficients by 45.26% and 35.79%, respectively, relative to the pre-stabilization period; 2) The displacement and deformation of the slope corresponding to the two reinforcement schemes have decreased significantly relative to the pre-reinforcement period, i.e., the coarse reinforcement measures in the schemes have produced effective reinforcement effects; 3) Considering comprehensively, Scheme 1 has more long-term stability benefits, and Scheme 2 has more economic benefits.

**Keywords:** Construction; Stability factor; Slip-resistant piles; Anchors; Reinforcement.

### 1. Introduction

Xinjiang is located in the hinterland of Asia and Europe continent, belongs to the oceanic arid zone, has unique natural geography and geological environment characteristics, the topography and geomorphology is “three mountains and two basins” pattern, the mountains and plains have a wide range of height difference. Special geological conditions and the acceleration of infrastructure construction have led to the formation of a large number of highway slopes in the rift valley, and the risk of slope destabilization has been gradually aggravated by the construction disturbances and climatic influences. Experts at home and abroad have also targeted a large number of correlation studies, which provide important technical references for slope risk analysis and reinforcement management [1-3]. Deng Shirong et al [4] proposed a widened anti-slip pile structure at the top of the embedded section, and deduced the formula for calculating its internal force, displacement, and ground reaction force; Lu et al [5] analyzed the effects of anchors with different burial depths, anti-slip piles of different depths, and anti-slip piles with different reinforcement locations on slope reinforcement; Zhang Gangxin et al [6-7] comparatively investigated the effect of slope reinforcement with different pile lengths, pile positions, and pile spacing based on the sensitivity analysis of characteristic parameters; FENG Zhen et al [8] proposed the optimal reinforcement scheme of h-type anti-slip piles based on different slope morphology and verified the feasibility by combining with practical engineering; ZHENG Qiyin et al [9] comparatively investigated the changes of slope stability under different anti-slip piles anchorage position and depth conditions; WANG Yankun et al [10] conducted a sensitivity study of the unreinforced, anchored, geogrid, anchored and geogrid slopes, respectively, based on the finite element model.

Anti-slip piles and anchors are widely used in various types of slopes as common reinforcement measures in slope reinforcement engineering. This paper takes a roadside slope in Xinjiang under the influence of construction disturbance as an example, and establishes a synergistic model of the

two types of support structures by comprehensively using finite element simulation, indoor and outdoor experiments, expert analysis and other methods. By comparing the performance of the two support systems of anti-slip piles and anchors in the dimensions of stress field, displacement field and program feasibility, it is found that Scheme 1 improves the slope stability coefficient by 45.26%, and Scheme 2 improves the slope stability coefficient by 35.79%. The research results form a technical path of “ data analysis - dynamic model construction - real-time program feedback” , which provides a reference for similar projects to make decisions that take into account both safety and economy.

## 2. Slope profile

The slope of this section is an excavation slope, belonging to the low to medium hill topography, with little undulation in the longitudinal topography, gentle transverse slope, low hill slope topography, and the overall slope direction is  $190^{\circ} \angle 47^{\circ}$  . No groundwater was found in the investigation area, the slope is gently sloping, the shallow layer is dominated by yellow-brown gravel soil, and pebbles are exposed underneath, and the slope disease is currently dominated by denudation and deformation, and there is a potential risk of instability due to the influence of heavy rainfall and construction, in order to prevent the slope from deformation and expansion, the main slide surface of the slope is determined through on-site investigation and expert analysis, as shown in Fig. 1.

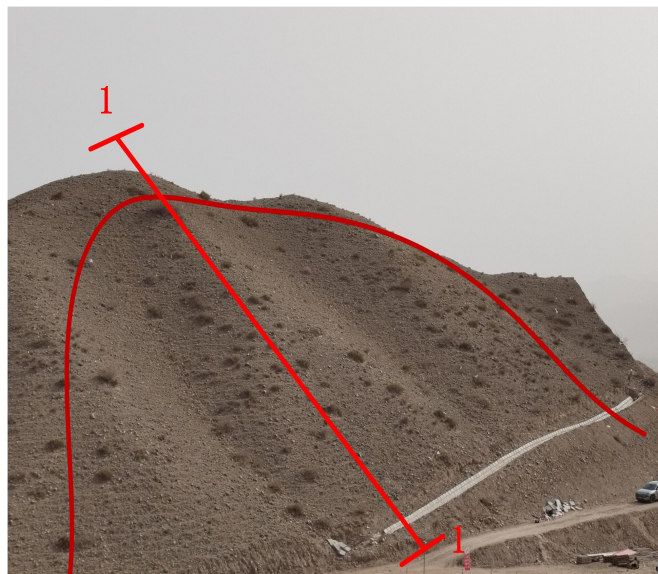


Fig. 1 Slope Main Slip Surface

## 3. Stability analysis

According to the results of field geological exploration to determine the main section of the slope geological structure as shown in Fig. 2, the slope surface layer covered with gravel soil, the bottom layer is pebble layer. Through indoor and outdoor experimental analysis and theoretical calculation, the main sliding geological structure and potential sliding surface of the slope are determined as shown in Fig. 2, and the physical and mechanical parameters of the geotechnical body are shown in Table 1.

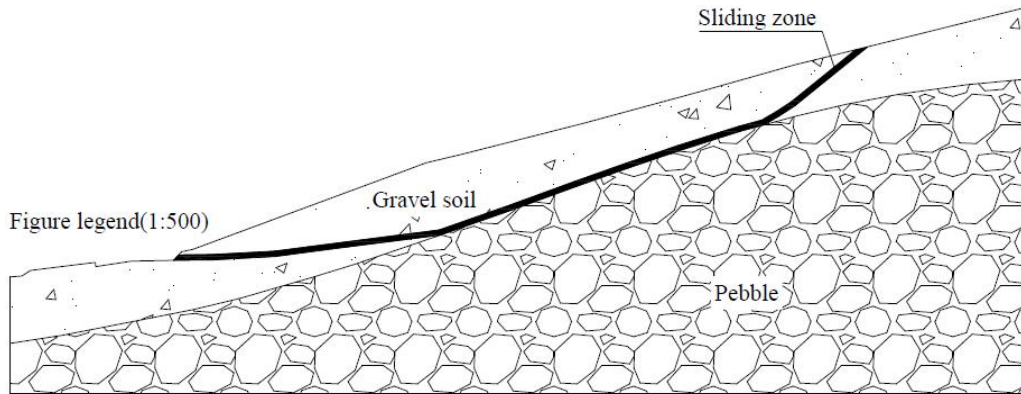


Fig.2 Geological structure of the potential main sliding surface

Table 1. Physical and mechanical parameters

Form	severe/(kN.m-3)	Cohesive force/kPa	Friction angle/(°)	Modulus of elasticity/MPa	Poisson's ratio
Sliding zone	18	21.5	16	14	0.3
Gravelly soil	20	16	20	20	0.32
Pebble	24	5	42	200	0.35
Pile	24	-	-	30000	0.2
Anchor rods	-	-	-	200000	0.35

Based on the geological structure of the main sliding surface, the finite element model is constructed as shown in Fig. 3, in which the x-axis direction of the coordinate system is horizontal, the y-axis direction is vertical, the z-axis direction is perpendicular to the xy-plane direction, the bottom surface of the model imposes the displacement constraints in the horizontal and vertical directions, and the horizontal displacement constraints are imposed on both sides of the model. Numerically analyze the stress field and displacement field of the main sliding surface of the slope, and get the corresponding average stress cloud as shown in Fig. 4, and the displacement cloud as shown in Fig. 5, take the top of the slope as the tracking research point, and take the inflection point of the displacement and deformation curve of the point as the judgment criterion of the slope instability, and get the curve of change of the stability coefficient of the slope as shown in Fig. 6.

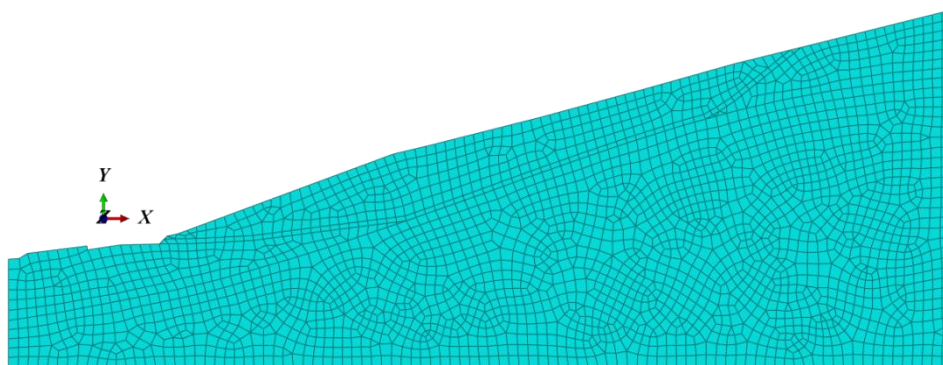


Fig. 3 Finite Element Model

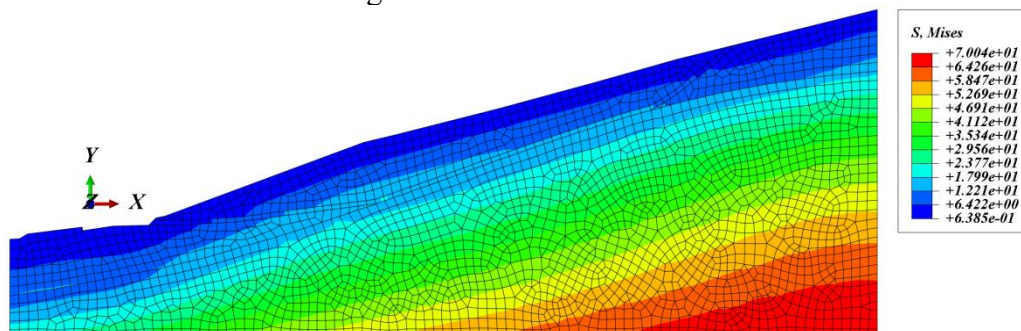


Fig. 4 Average stress contour

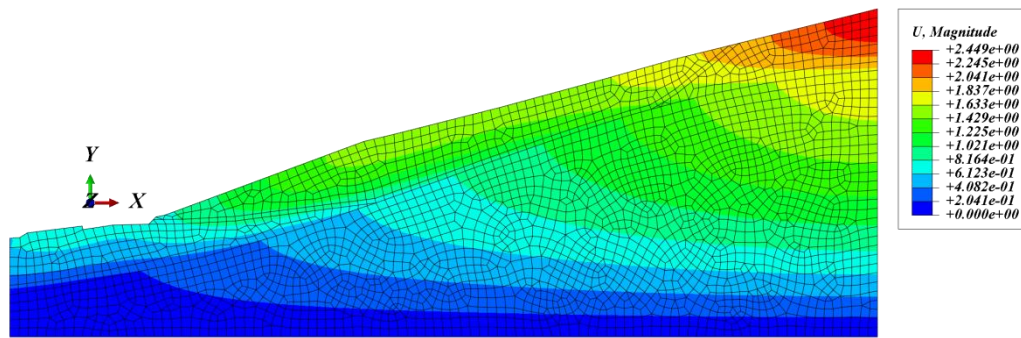


Fig. 5 Displacement contour

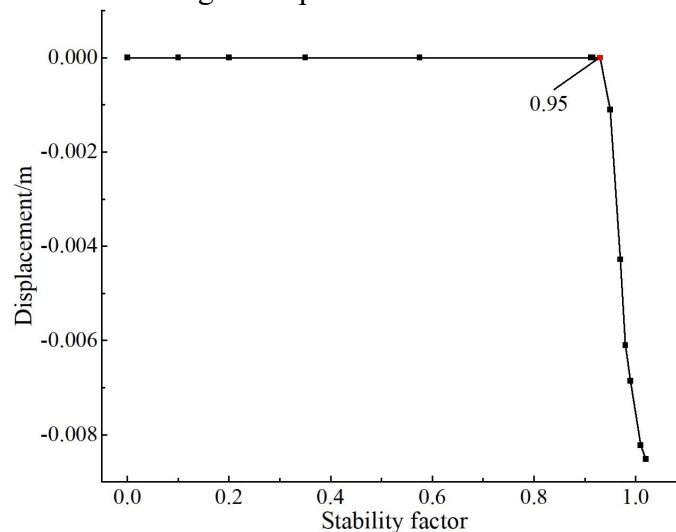


Fig. 6 Stability coefficient variation curve

It can be seen from Fig. 4 and 5 that the average stress of the main sliding surface increases uniformly in layers along the slope direction from the surface layer of the slope to the interior of the slope. The average stress of the surface gravel soil is the smallest, about 0.64kPa, and the average stress at the bottom of the slope is the largest, about 70.04kPa. The distribution form of the slope displacement decreases layer by layer from the top of the slope to the foot of the slope. The displacement deformation of the top of the slope is the largest, about 2.45mm, and the displacement deformation of the foot of the slope is the smallest.

As can be seen from Fig. 6: the slope tracking research point displacement in the x-axis of 0.95 when a sudden change occurs, that is, the slope destabilization occurs, to determine the stability coefficient of the slope is 0.95. The specification requirements of such slopes in the natural conditions of the stability coefficient is not less than 1.01, that is, the current stability status of the slope does not meet the requirements of the existence of the risk of destabilization, the need to take measures to strengthen the management.

#### 4. Reinforcement

Combined with the results of site investigation and slope stability analysis, two reinforcement schemes were developed for the main sliding surface of the slope, the specific layout is shown in Fig. 7 and Fig. 8, and the physical and mechanical parameters of the reinforcement materials are shown in Table 1. Scheme 1 is: circular anti-slip piles + anchors + intercepting drainage, in which the pile section radius is 0.9m, pile spacing is 2m, pile length is 7m, the upper pile embedded section of the slope is 5m long, and the lower pile embedded section is 5.2m long; the diameter of the 5m long anchors is 130mm, and the laying spacing is 3m, with the horizontal inclination angle

of  $30^\circ$  ; the diameter of the 4.5m long anchors is 130mm, with the laying spacing of 3m, with the horizontal inclination angle of  $45^\circ$  ; build water interceptor ditches at the top of the slope and both sides of the slope. Scheme 2 is: square anti-slip piles + intercepting and draining, of which the pile section is  $2 \times 3\text{m}$ , the layout spacing is 2m, the pile length is 7m, and the embedded section length is 5.5m; build intercepting ditches at the top of the slope and on both sides of the slope.

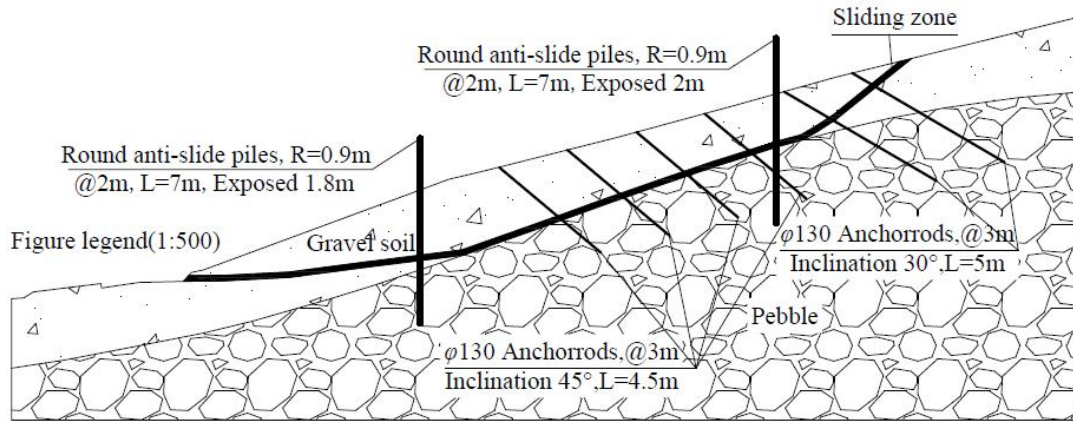


Fig. 7 Schematic diagram of the layout of Scheme 1

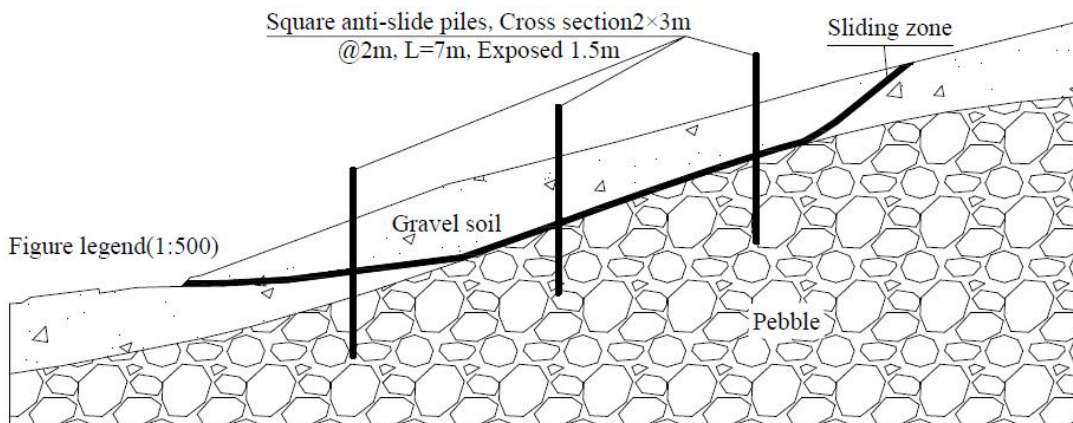


Fig. 8 Schematic diagram of the layout of Scheme 2

Based on the design of the two reinforcement schemes, the finite element models corresponding to the reinforcement schemes are constructed as shown in Fig. 9 and Fig. 10, respectively, in which the anti-slip piles are added by the beam component and meshed by the B21 cell type, and the anchors are added by the truss component and meshed by the T2D2 cell type; the anti-slip piles and the anchors are embedded with embedded constraints in the interior of the slope body, and the horizontal and vertical displacement constraints are imposed on the bottom surface of the model, and the horizontal displacement constraints are imposed on the two sides of the model.

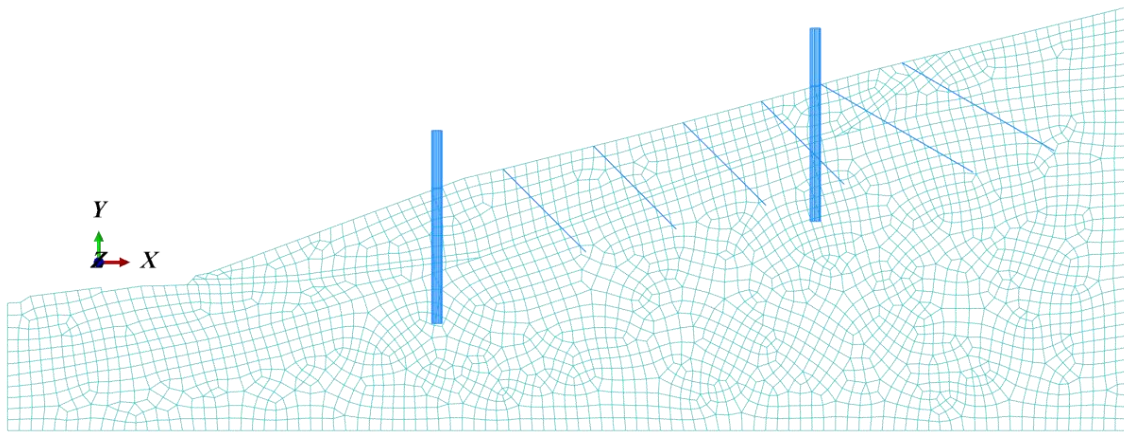


Fig. 9 Finite element model of scheme 1

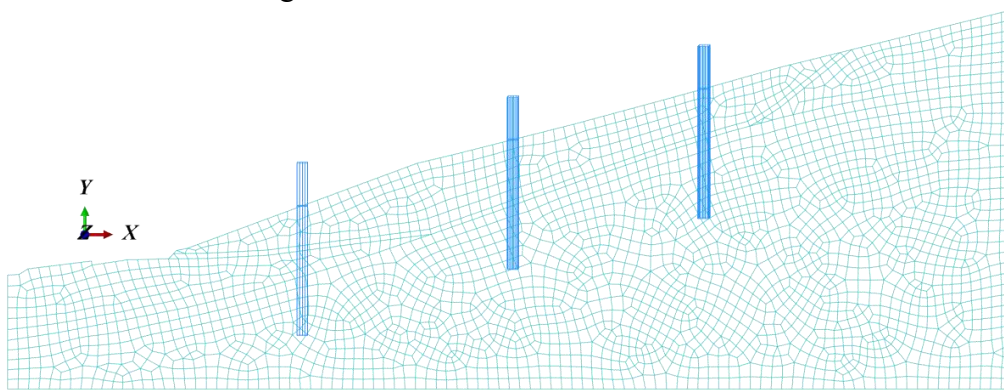


Fig.10 Finite element model of scheme 2

Numerical calculations yielded the average stress cloud and displacement cloud for Scheme 1 as shown in Fig. 11 and Fig. 12, and for Scheme 2 as shown in Fig. 13 and Fig. 14.

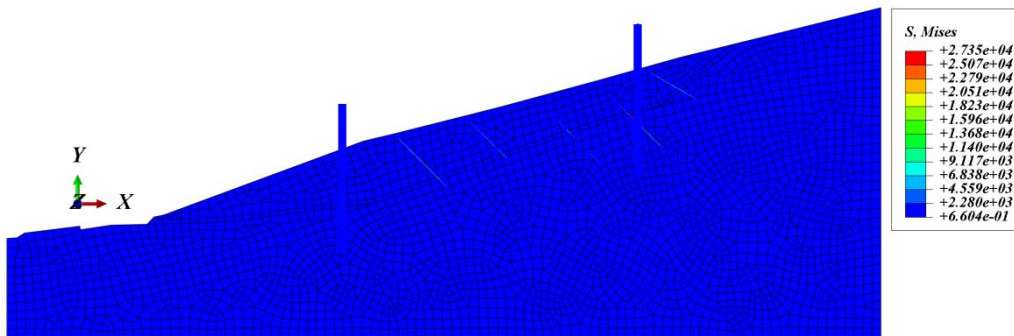


Fig. 11 Average stress contour of scheme 1

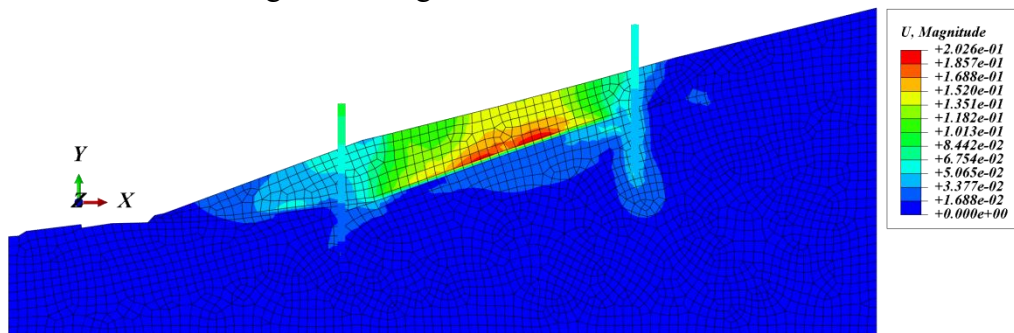


Fig. 12 Displacement contour of scheme 1

As can be seen from Fig. 11 and Fig. 12: the maximum average stress is  $2.74 \times 10^4$  kPa, mainly concentrated in the anchor and its surrounding area, indicating that the anchor produces an effective

slip-resisting effect; the minimum average stress is 0.66kPa, mainly concentrated in the interior of the slope body; the maximum displacement is 0.2mm, mainly concentrated in the area of gravel soil in the surface layer of the slope body, and the displacement is reduced by 91.84% relative to that before the reinforcement. Indicating that the reinforcement measures have produced a reinforcing effect, and the deformation and damage of the slope is effectively controlled.

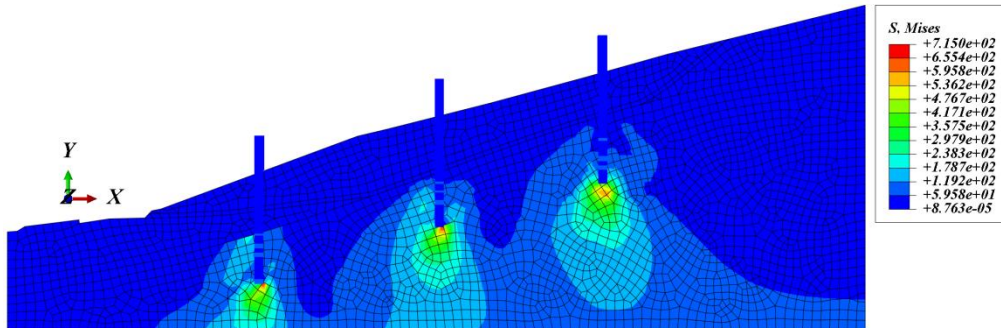


Fig. 13 Average stress contour of scheme 2

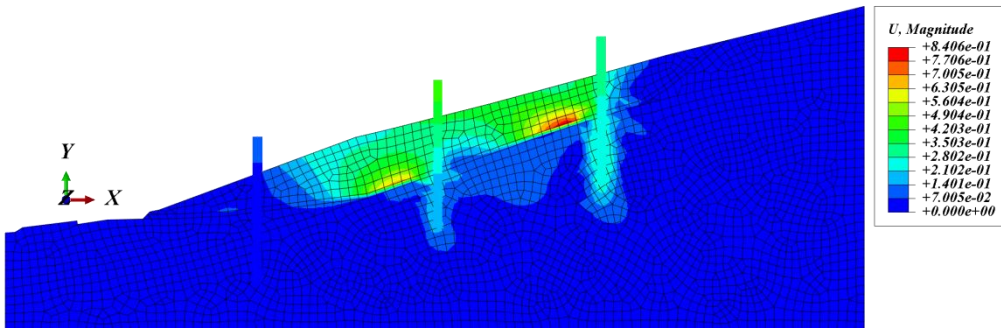


Fig. 14 Displacement contour of scheme 2

As can be seen from Fig. 13 and Fig. 14: the maximum average stress is  $7.15 \times 10^2$  kPa, mainly concentrated in the contact position between the bottom of the anchor and the slope body, indicating that the anchor has produced an effective slip-resisting effect for preventing the deformation of the slope body from being broken; the minimum average stress is  $8.76 \times 10^{-5}$  kPa, mainly concentrated in the interior of the slope body; the maximum displacement is 0.84mm, mainly concentrated in the area of gravel soil in the surface layer of the slope body. The displacement was reduced by 65.71% relative to the pre-strengthening displacement, but enhanced by 320% relative to Scheme 1, indicating that the reinforcement measures produced effective reinforcement, but relatively weaker than the reinforcement effect of Scheme 1.

The tracking research point consistent with the pre-reinforcement is selected, and the displacement mutation at this point is used as the judgment standard of slope instability, and the change curves of slope stability coefficients corresponding to the two reinforcement schemes are obtained through numerical analysis as shown in Fig. 15.

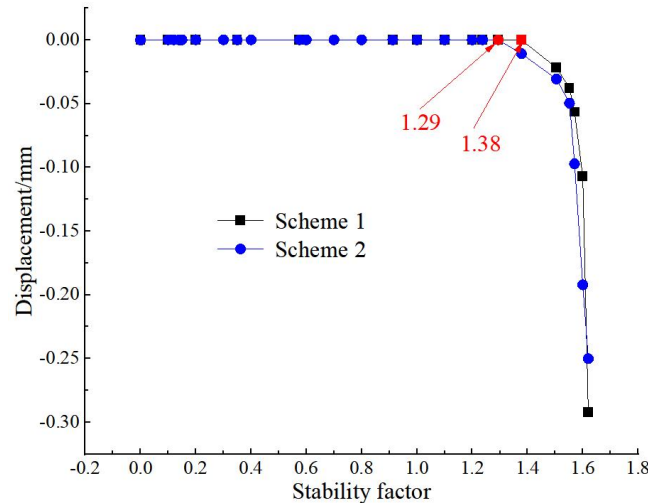


Fig. 15 Variation curve of stability coefficient of reinforcement scheme

As can be seen from Fig. 15: the slope stability coefficient corresponding to Scheme 1 is 1.38, which is 45.26% higher than that before reinforcement, and the slope stability coefficient corresponding to Scheme 2 is 1.29, which is 35.79% higher than that before reinforcement, and 6.52% lower than that of Scheme 1; both reinforcement programs satisfy the stability requirements of the code for this type of slopes, and both of them improve the stability of the slopes effectively.

## 5. Summary

(1) The displacement and deformation of scheme 1 is 91.84% lower than that before slope stabilization, and the stability coefficient of the slope is 45.26% higher, and the anti-slip piles and anchors in the scheme have effective stabilization effect, which meets the stabilization requirements of the slope.

(2) The displacement and deformation of scheme 2 is reduced by 65.71% relative to the slope before reinforcement, and the slope stability coefficient is improved by 35.79%, and the anti-slip pile in the scheme produces effective reinforcement, which meets the reinforcement requirements of the slope.

(3) Both reinforcement schemes meet the requirements of slope reinforcement, from the perspective of economic cost and construction difficulty, scheme 2 is recommended as the most suitable reinforcement program; from the perspective of long-term stability, scheme 1 is recommended as the most suitable reinforcement program.

## Acknowledgments

This work was financially supported by National Key R&D Project (2022YFC3002603), Chongqing Natural Science Foundation Upper-level Project (CSTB2023NSCQ-MSX0878), Major Science and Technology Special Project/Key R&D Task Special Project of the Autonomous Region (2022B03033-2).

## References

- [1] Wang Chongjing, Zhang Long, Liu Guowei. Comprehensive evaluation of soil slope stability by combining fuzzy mathematical judgment and numerical simulation. Chinese Journal of Geological Hazards and Prevention, 2023, 34(6):69-76.
- [2] Xu Shumei, Xiao Lin, Li Chengcheng, et al. Status review on two kinds of typical geological hazard zoning techniques in China. Journal of Natural Disasters, 2017, 26(2): 22-31.

- [3] Dai Xuan, Ma Yunxiang, Wei Shaowei, et al. Seismic performance analysis of new assembled anchor cable frame beam reinforced slopes under different seismic intensities. *Journal of Geotechnical Engineering*, 2023, 45(S2): 147-152.
- [4] Deng Shirong, Xiao Shiguo. Calculation method of widened anti-slip pile at the top of embedded section. *Chinese Journal of Geological Hazards and Prevention*, 2022, 33(4): 84-91.
- [5] Lu Beisi, Song Fei, Jin Yangtao, et al. Stability analysis and reinforcement technology study of a highway slope in cambodia. *Hans Journal of Civil Engineering*, 2021, 10(5): 419-427.
- [6] Zhang Bangxin, Jia Jianqing, Liu Zhongshuai, et al. Stability analysis of Xiafen slope and its management measures. *Lanzhou Jiaotong University Journal*, 2023, 42(1): 9-15.
- [7] Zhang Bangxin, Peng Dongming, Tan Ling, et al. Numerical analysis and reinforcement management of landslide on a highway in Zhangzhou, Fujian. *Drilling Engineering*, 2024, 51(4): 117-124.
- [8] Feng Zhen, Wang Boyi, Liu Haoran, et al. Analysis of reinforcement effect of h-type anti-slip pile based on slope morphology. *Science, Technology and Engineering*, 2022, 22(30): 13467-13476.
- [9] Zheng Qiyin. Analysis of anchorage position and depth of skid pile based on Midas/GTS. *China Highway*, 2022, 12(20): 118-120.
- [10] Wang Yankun, Song Ling, Liu Jie, et al. Finite element numerical analysis of slope protection by anchor-geocell composite structure. *Highway*, 2021, 66(11): 20-26.